Proceedings of the IASS 2024 Symposium
Redefining the Art of Structural Design
August 26-30, 2024, Zurich Switzerland
Philippe Block, Giulia Boller, Catherine DeWolf,
Jacqueline Pauli, Walter Kaufmann (eds.)

Optimization Study on Double Layer Cable System Structure of Marine Photovoltaic Power Generation Support

Gaoming Zhang*, Zhaoxu Shen, Ming Ma

*China Academy of Building Research
30 North 3rd Ring East Road, Chaoyang District, Beijing, China
zhanggaoming@cabrtech.com

Abstract

A certain photovoltaic power generation project adopts a double-layer cable flexible support structure, with the lower chord cable as the load-bearing cable and the upper chord cable as the stabilizing cable. The upper and lower chord cables are connected through triangular supports between cables, and the two cable trusses are connected by cross braces between cables. Both the high and anchor piles are prestressed concrete pipe piles. The wind load of the flexible photovoltaic support structure is the control load, and the value of its shape coefficient should be studied in detail. Wind pressure loading can also be carried out based on the results of wind tunnel experiments. The ice load and wave load of the flexible photovoltaic support structure are special and important forms of load for this structure, which need to be calculated based on the average hydrological conditions of the sea area over the years. Due to the deep silt layer on the mudflat in the sea area, the horizontal bearing capacity of the pile foundation of the flexible photovoltaic support is low. The horizontal stability and pile length of the pile foundation should be considered according to the embedded stability of the cantilever retaining structure. This flexible bracket structure system greatly improves the span length of photovoltaic brackets, allowing for the development of fisheries and aquaculture, and the full utilization of land resources. It is currently widely used as a type of photovoltaic bracket system.

Keywords: Photovoltaic power generation, double-layer cable system, flexible support, ice load, marine photovoltaic.

1. Introduction

A certain photovoltaic power generation project is located in Huanghua City, Hebei Province. It mainly utilizes the enclosed aquaculture water surface and some sea areas for the construction of complementary photovoltaic projects for fishing and light. The current site is enclosed aquaculture ponds and sea areas, with an elevation of about -2 to 5 meters. The land comprehensive utilization and development method of this photovoltaic project is "complementary fishing and light". Under the photovoltaic modules, modern fishing and breeding industries are developed according to regional conditions, which not only releases industrial production capacity and saves enterprise costs, but also develops fishing and breeding industries, fully utilizing land resources. Through this approach, not only can the local abundant solar energy resources be effectively utilized, but it also has a positive effect on improving the ecological environment of the site and increasing the value of land use.

2. Flexible support structure system for photovoltaic power generation

This project adopts a double-layer cable flexible support structure, with a single span of 35832mm. The lower chord cable is the load-bearing cable, and the upper chord cable is the stable cable. The ultimate strength standard value of the steel strand is 1960N/mm^2. The upper chord cables are arranged horizontally, and the lower chord cables are deflected by 1800mm (the height of the cable truss); The

upper and lower chords are connected by triangular supports between cables, and the two cable trusses are connected by cross braces between cables; The end high pile crossbeam and the middle high pile crossbeam are made of hot-rolled H-shaped steel; The middle high pile adopts pre-stressed concrete pipe piles, which are arranged in a staggered manner. The end high pile also adopts pre-stressed concrete pipe piles, which are arranged in accordance with the cable truss. End anchor piles, for aquaculture areas, are used to anchor the diagonal pull rods that extend from the high end pile crossbeam in the form of one cable and one pile; For the sea area, the form of two cables and one pile is used to anchor the diagonal pull rod that extends from the high pile beam at the end. Anchor piles and cable trusses are arranged according to the corresponding frame, and prestressed concrete pipe piles are used. The side view (partial) of the double-layer cable system is shown in Figure 1, the pile arrangement is shown in Figure 2, the transverse component arrangement is shown in Figure 3, and the cable truss arrangement is shown in Figure 4.

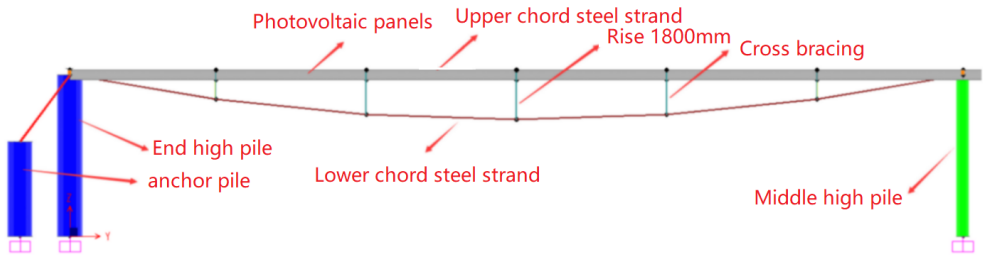

Fig. 1 Side view of double-layer cable system structure for photovoltaic power generation

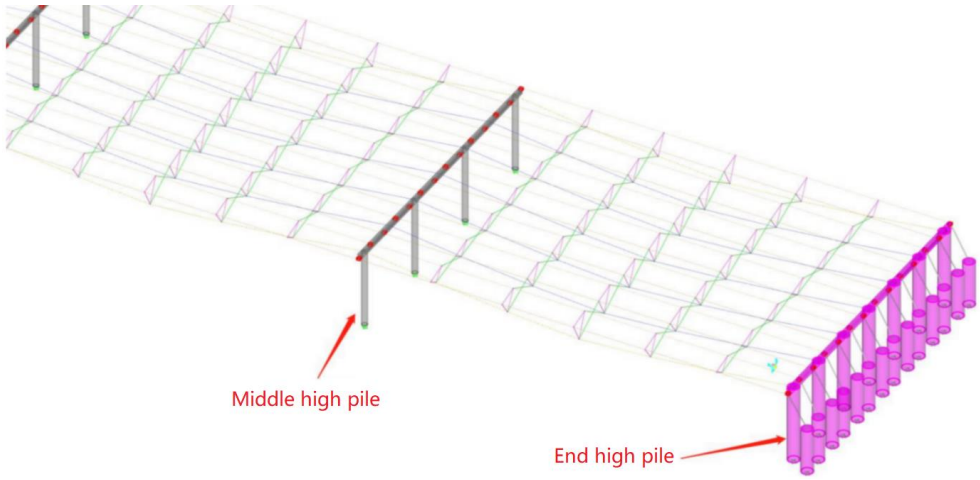

Fig. 2 Layout diagram of double layer cable system structure piles for photovoltaic power generation

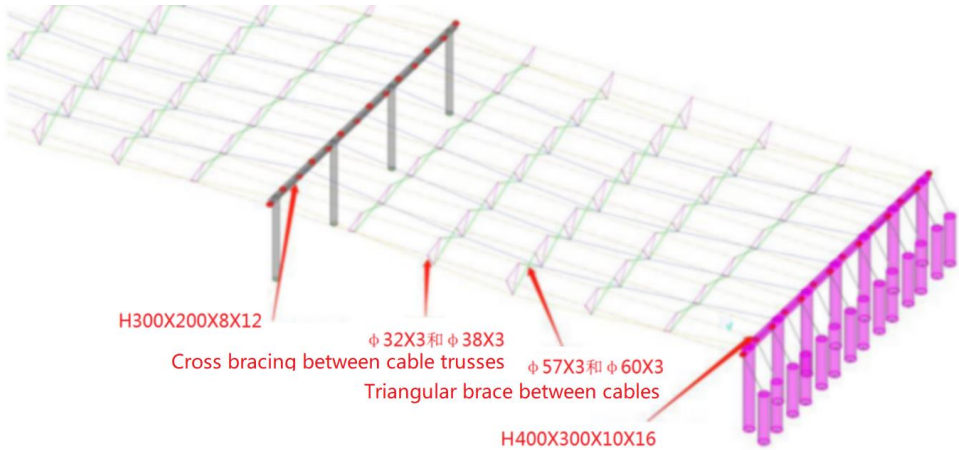

Fig. 3 Layout of Horizontal Bars for Double Layer Cable System Structure in Photovoltaic Power Generation

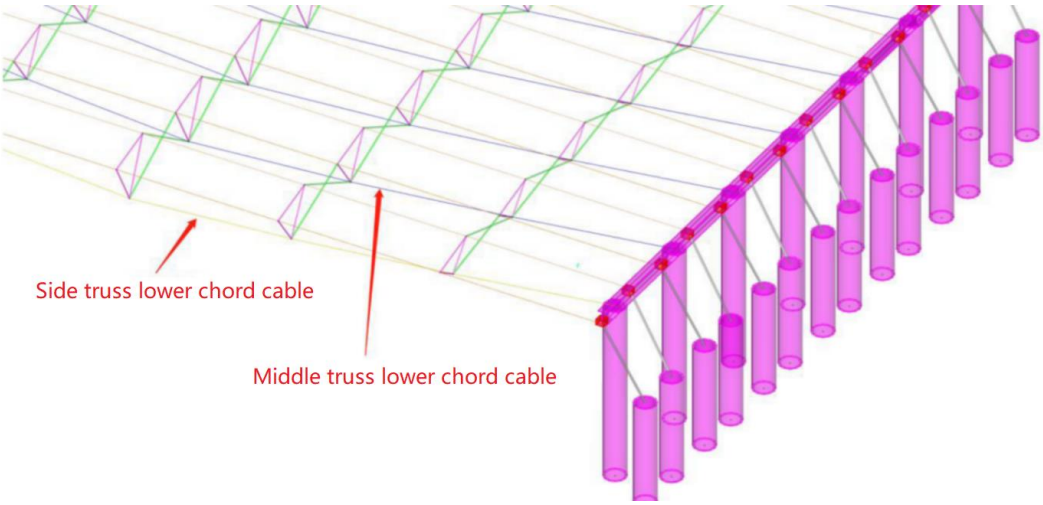

Fig. 4 Layout diagram of double layer cable truss structure for photovoltaic power generation

3. Wind load values for photovoltaic power generation brackets

Wind load shape coefficient μ_s. According to the "Design Specification for Photovoltaic Support Structures" NB/T10115-2018, the body shape coefficient is taken as 0.8. For large-area photovoltaic support structures, the body shape coefficient of the middle module located inside is reduced, and the body shape coefficient of the edge module located outside is not reduced.

According to item 4.1.3 of the "Design Specification for Photovoltaic Support Structures" NB/T10115-2018, when the photovoltaic panel array is arranged with more than 7 rows, the support body shape coefficient within the second and fourth rows of both ends can be reduced. The reduction coefficient can be taken as 0.85. The average positive pressure body shape coefficient after this should not be less than 0.6, and the average negative pressure body shape coefficient should not be greater than -0.9.

For the maximum average wind coefficient (positive wind pressure), consider it as follows.

Wind force coefficient without considering reduction.

$$Cp=\mu_{s1}\mu_z=0.8\times1.1546=0.9237 \quad (1)$$

Consider the wind force coefficient when reducing.

$$Cp=\mu_{s1}\mu_z=0.8\times0.85\times1.1546=0.7851 \quad (2)$$

For the minimum average wind coefficient (negative wind pressure), consider it as follows.

Wind force coefficient without considering reduction.

$$Cp=\mu_{s1}\mu_z=-0.95\times1.1546=-1.0969 \quad (3)$$

Consider the wind force coefficient when reducing.

$$\mu_{s1}=\min(-0.95\times0.85，-0.9) =-0.9 \quad (4)$$

$$Cp=\mu_{s1}\mu_z=-0.9\times1.1546=-1.0391 \quad (5)$$

This project adopts the wind force coefficient obtained from wind tunnel experiments for loading. Envelope statistics were performed on the wind tunnel test results of 36 wind directions to obtain the statistical values of the wind coefficient on the photovoltaic panel under parallel interference conditions (adjacent specimens were set at the parallel position of the test specimens to simulate real turbulence). Then, the wind coefficient on a panel was weighted and averaged using a center point weight of 0.5+edge point weight of 0.125, resulting in the positive wind pressure wind coefficient distribution diagram shown in Figure 5 and the negative wind pressure wind coefficient distribution diagram shown in Figure 6.

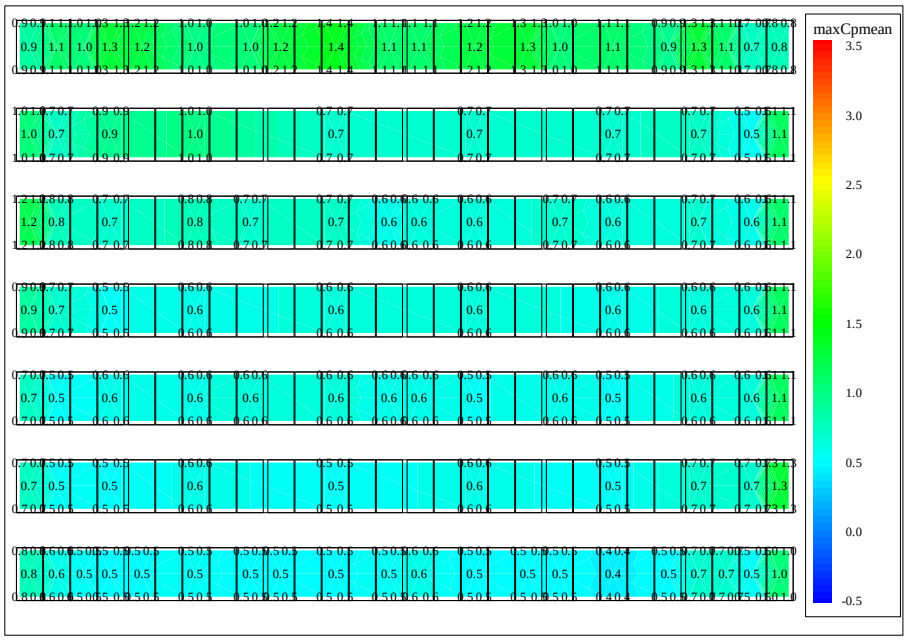

Fig. 5 Distribution map of positive wind pressure and wind coefficient

For the distribution of wind force coefficients under positive wind pressure in wind tunnel experiments, if the wind force coefficients of the two beams in front of the wind are greater than the specifications, they will be loaded according to the results of wind tunnel experiments. This area is called the edge beam; The wind force coefficients of the following multiple beams are equivalent to the standard values, and are loaded according to the standard. This area is called the middle beam.

For the distribution of wind force coefficients under negative wind pressure in wind tunnel experiments, if the wind force coefficients of the two beams in front of the wind are greater than the specifications, the loading should be carried out according to the results of wind tunnel experiments, and this area is called the edge beam; The wind coefficient of several subsequent beams is smaller than the specified value. They were loaded according to the specifications and reduced to 0.9 according to the provisions of item 3.4.9 of the Standard Wind Tunnel Test Methods for Building Engineering. This area is called the middle beam.

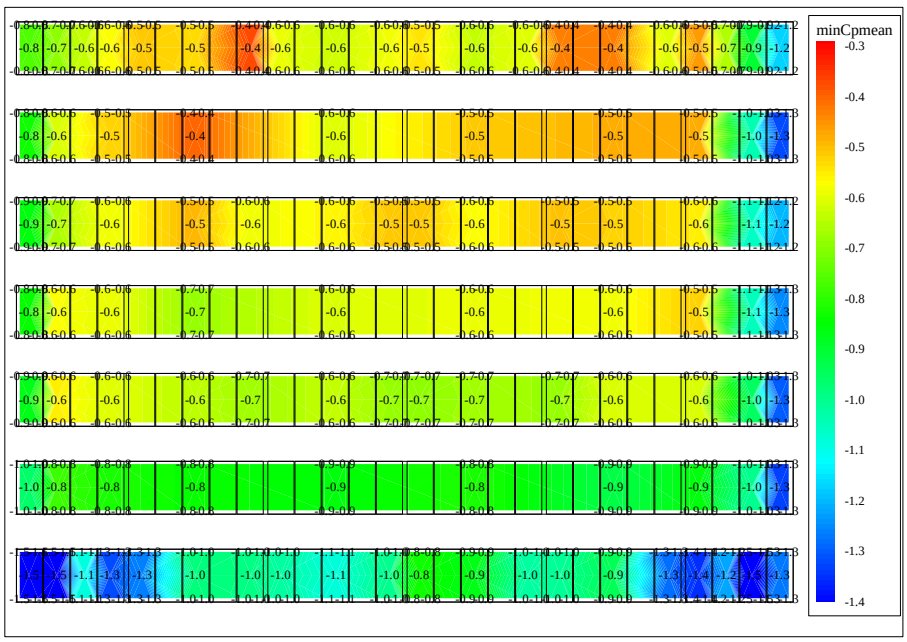

Fig. 6 Distribution map of negative wind pressure wind coefficient

4 Ice load value of photovoltaic power generation bracket

This project adopts the design water level of Huanghua Port Station as the calculated water level in the project area. Under the 1985 national elevation benchmark, the high tide level of the engineering area is 3.21m for a 50 year high tide, 3.02m for a 25 year high tide, 2.45m for a 2 year high tide, 1.75m for a design high tide, and -1.86m for a design low tide. When designing low tide levels, with a recurrence interval of 2 years, a recurrence interval of 25 years, and a recurrence interval of 50 years, all the engineering areas are exposed to the beach.

The tidal current in the engineering sea area is mainly semi diurnal, and the form of tidal movement has a certain degree of rotation. From the measured ocean currents, it can be seen that the current intensity in the engineering sea area is not significant; The average maximum vertical flow velocity of rising and falling tides is between 0.26m/s and 0.46m/s, and the average flow velocity is between 0.1/s and 0.3m/s. Due to the small water depth (which is in an exposed state during average low tide levels), the difference in surface and bottom flow velocities is not significant. The general flow direction of rising and falling tides is in the SW-NE direction. According to actual measurements, the possible maximum flow velocity of the tidal current outside the project is 0.51m/s, flowing towards 230 °.

Based on the average ice thickness over the years, calculate the average ice thickness for different return periods. The design ice thickness for different return periods is shown in Table 1. The results obtained by fitting Pearson-III probability distribution function and Weibull probability distribution function are roughly the same, and the average of the two is used as the design value for different return periods.

Based on the above analysis, the following conclusions can be drawn that the thickness of flat ice in the engineering sea area is about 31cm once every 50 years, 27cm once every 25 years, and 8cm once every 2 years.

Tab. 1 Design Ice Thickness of Flat Ice at Different Return Periods in the Engineering Sea Area

Return period	1 year	2 year	5 year	10 year	20 year	25 year	50 year	100 year
Pearson-III type Flat ice thickness (cm)	2.0	7.4	14.5	20.0	24.4	25.9	30.7	35.4
Weibull Flat ice thickness (cm)	2.2	7.9	16.1	21.2	25.8	27.2	31.4	35.4
Average Flat ice thickness (cm)	2.1	7.7	15.3	20.6	25.1	26.6	31.1	35.4

The flat design ice thickness for different return periods in the Bohai Sea, Liaodong Bay, and Laizhou Bay sea areas is shown in Table 2.

Tab. 2 Design Ice Thickness of Flat Ice at Different Return Periods in the Liaodong Bay and Laizhou Bay Seas

Return period	1 year	2 year	5 year	10 year	20 year	25 year	50 year	100 year
West Coast of Liaodong Bay(cm)	6.8	15.4	22.4	27.5	31.4	32.0	36.2	41.0
laizhou bay(cm)	1.8	-	14.0	19.0	23.5	-	29.8	34.3

For the peripheral protective piles, the main consideration is the compressive ice force of ice. According to the "Design Regulations for Steel Fixed Platforms in Bohai Sea" Q/HSn3003-2002, the design load of ice is considered based on a 50 year return period. According to the "China Sea Ice Conditions and Application Regulations" Q/HSn3000-2002, the compressive strength of sea ice is taken as 2.03MPa, and the design thickness of a single layer of ice is taken as 39.5cm.

The calculation of ice compression force is as follows.

$$If_c = 3.57h^{0.1} / D^{0.5} = 3.57 \times 39.5^{0.1} / 120^{0.5} = 0.471 \tag{6}$$

$$F = mIf_c \sigma_c Dh = 0.9 \times 0.471 \times 2.03 \times 10^6 \times 0.395 \times 1.2 = 407.9\text{kN} \tag{7}$$

For the internal piles, the main consideration is the impact force of the flowing ice after being cut by the peripheral protective piles. The net distance of the peripheral protection pile is 3.8m, and it is considered

that the maximum size of floating ice entering the interior of the peripheral protection pile is 3.8m× 3.8m of flowing ice. When calculating the force of flowing ice, the collision energy method in "Analysis and Determination of Ice Load in Bohai Sea" is used, which means that all the kinetic energy of ice load movement is converted into the deformation of the pile. According to the "Regulations on the Conditions and Application of Sea Ice in China" Q/HSn3000-2002, the mass density of sea ice is 850kg/m^3, the flow velocity of floating ice is 0.6m/s, and the thickness of floating ice is 39.5cm.

The collision force of flowing ice is calculated as follows.

The kinetic energy of ice movement is calculated using the following formula.

$$m = \rho tA = 850 \times 0.395 \times 3.8 \times 3.8 = 4848.23\text{kg} \tag{8}$$

$$E_{\mathrm{k}} = 1/2 \cdot kmv^2 C_{\mathrm{m}} = 1/2 \times 1 \times 4848.23 \times 0.6^2 \times 1.4 = 1221.754\text{N} \cdot \text{m} \tag{9}$$

The energy generated by collision force deformation is calculated using the following formula.

$$E_{\mathrm{S}} = 1/2 \times FD = 1221.754\text{N} \cdot \text{m} \tag{10}$$

Iteration can be used to determine the force exerted by the floating ice on the structure.

5 Wave load values for photovoltaic power generation brackets

According to section 10.3 of the Port and Waterway Hydrological Code JTS145-2015, the wave load is calculated according to items 10.3.2 to 10.3.5 for small diameter piles in deep water. For small-scale piles, the maximum velocity component P_{Dmax} and maximum inertia component $P_{1\mathrm{max}}$ acting on the entire pile height should be determined according to the following regulations.

$$P_{D\max} = C_D \frac{\gamma D H^2}{2} K_1 \tag{11}$$

$$P_{1\max} = C_M \frac{\gamma A H}{2} K_2 \tag{12}$$

$$K_1 = \frac{\frac{4\pi z_2}{L} - \frac{4\pi z_1}{L} + sh\frac{4\pi z_2}{L} - sh\frac{4\pi z_1}{L}}{8\mathrm{sh}\frac{4\pi d}{L}} \tag{13}$$

$$K_2 = \frac{sh\frac{2\pi z_2}{L} - sh\frac{2\pi z_1}{L}}{\mathrm{ch}\frac{2\pi d}{L}} \tag{14}$$

Where, H—Wave height measurement at the location of the building(m)；

d—Water depth in front of the building(m)；
L—Wavelength(m)；
z_1、z_2—Calculate the height of the point above the water bottom(m)；
γ—The gravity of water(kN/m^3)；
A—The cross-sectional area of the pile body(m^2)；
D—The diameter of the pile body(m)；
C_D—Speed force coefficient, taken as 1.2 for circular cross-section；
C_M—Inertia force coefficient, taken as 2.0 for circular cross-section.
For small-scale piles, the maximum total wave force acting on the entire pile height can be determined using the following method.

(1) When $P_{\mathrm{Dmax}} \leq 0.5P_{1\mathrm{max}}$, the maximum total horizontal wave force in the forward direction is $P_{\mathrm{max}} = P_{1\mathrm{max}}$.

(2) When $P_{\mathrm{Dmax}}>0.5P_{1\mathrm{max}}$, the maximum total horizontal wave force in the forward direction is shown below.

$$P_{\max}=P_{D\max}\left(1+0.25\frac{P_{1\max}^2}{P_{D\max}^2}\right) \tag{15}$$

Where, P_{Dmax} and $P_{1\mathrm{max}}$ are the maximum velocity component and maximum inertia component acting on the entire pile height, respectively.

6 Research on pile foundation stability

According to item 4.2.1 of the Technical Regulations for Building Foundation Pit Support JGJ120-2012, the embedded depth (l_{d}) of cantilever support structures should meet the requirements for embedded stability as follows.

$$\frac{E_{pk}a_{p1}}{E_{ak}a_{a1}}\geq K_e \tag{16}$$

Where, E_{ak} and E_{pk} represent the standard values of active soil pressure on the outer side of the foundation pit and passive soil pressure on the inner side of the foundation pit, respectively. a_{a1} and a_{p1} represent the distance from the combined action point of active soil pressure on the outer side of the foundation pit and passive soil pressure on the inner side of the foundation pit to the bottom of the retaining member.

According to item 8.3.15 of the Design Code for Photovoltaic Support Structures (NB/T10115-2018), the overall stability verification of micro pile foundations should comply with the following provisions.

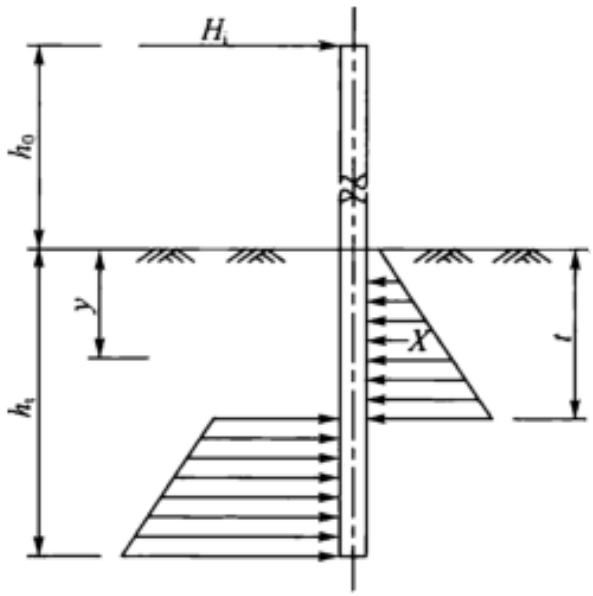

Fig. 7 Calculation diagram of overall stability of pile foundation

The verification should meet the following requirements.

$$R_H\geq K_{M_w}H_i \tag{17}$$

Where, R_{H} is the overall stability calculation horizontal resistance (kN) of the micro pile foundation, H_{i} is the horizontal force acting on the top of the micro pile foundation under the corresponding standard combination (kN), and K_{Mw} is the stability coefficient.

The overall stability verification of pile foundation and the horizontal resistance should be calculated using the following formula.

$$R_H=mb_0h_t^2/\left(\eta\mu_{cm}\right) \tag{18}$$

$$\eta = h_0 / h_t \tag{19}$$

$$\mu_{cm} = 3/\left(1-2\theta^3\right) \tag{20}$$

$$\theta = t / h_t \tag{21}$$

Where, m is the soil pressure parameter, which is calculated using the following formula.

$$m = \gamma_s \tan^2\left(45^\circ + \frac{\beta}{2}\right) \tag{22}$$

b_0 is the calculated width of the micro pile foundation, h_t is the burial depth of the micro pile foundation, η is the ratio of the horizontal force at the pile top to the design ground height and the burial depth of the micro pile foundation, μ_{cm} is the friction coefficient between the micro pile foundation and the soil contact area, h_0 is the distance from the H_i action point to the design ground, θ is the angle between the foundation pressure diffusion line and the vertical line, and is calculated using the following formula.

$$\theta^3 + \frac{3}{2}\theta^2\eta - \frac{3}{4}\eta - \frac{1}{2} = 0 \tag{23}$$

7 The load-bearing capacity of photovoltaic support cable system cables

According to Appendix A of the Code for Design of Concrete Structures (GB50010), a (1×7) standard steel strand with a diameter of 15.2mm has a nominal diameter of 15.2mm, a nominal cross-sectional area of 140mm2, and a breaking force of approximately 140kN.

All cable forces are subjected to ultimate state verification of bearing capacity according to the load combinations in Section 2.3. The control indicators for the bearing capacity of prestressed steel strands under each design basic combination are as follows.

According to Section 5.6 of the Technical Specification for Cable Structures (JGJ257-2012), the bearing capacity of cables should meet the following formula requirements.

$$F = \frac{F_{tk}}{\gamma_R} \tag{24}$$

Where, F—The tensile design value of the cable(kN);

F_{tk}—The ultimate tensile strength standard value of cables(kN);

γ_R—The partial coefficient of resistance for Lasso, taken as 2.0. When it is a steel tie rod, take 1.7.

$$\gamma_0 N_d \le F \tag{25}$$

Where, N_d—Design value of maximum axial tensile force borne by the cable(kN);

γ_0—Importance coefficient of structure.

According to item 5.2.5 of the Technical Specification for Glass Curtain Wall Engineering (JGJ102-2013), the bearing capacity of the cable should meet the following formula requirements.

In point supported glass curtain walls, the strength design values of tension rods and cables should be adopted according to the following regulations.

(1) The tensile strength design value of stainless steel tie rods should be determined by dividing their yield strength standard value $\sigma_{0.2}$ by a coefficient of 1.4

(2) The design value of tensile strength for high-strength steel strands or stainless steel strands should be calculated by dividing the standard value of their ultimate tensile bearing capacity by a coefficient of 1.8, and converted based on their equivalent cross-sectional area before use. When the standard value of the ultimate tensile bearing capacity of steel strands is known, the design value of their tensile bearing capacity should be taken by dividing this value by a coefficient of 1.8.

Based on the provisions of the above two specifications, the stress state of the cables in this project is more inclined towards structural tension, so the resistance sub factor is taken as 2.0.

8 Conclusion

After optimization research, this project adopts a double-layer cable system structure with a single span of 35832mm and a spacing of 3.80m. For the middle beam (areas with small wind loads), both the upper and lower chord cables are used φ 15.2 Steel strands, for the upper chord cables of edge trusses (areas with high wind loads) φ 15.2 Steel strands, bottom chord cable used φ 17.8 steel strands, with a standard ultimate strength value of 1960N/mm^2. Diagonal pull rod adopts φ 40 solid steel tie rods. The upper chord cables are arranged horizontally, and the lower chord cables are deflected by 1800mm (the height of the cable truss); The upper and lower chords are connected by support rods, and the triangular support between the cables is adopted φ 32×3 and φ 38×3 seamless steel pipe, with cross bracing between beams φ 57×3 and φ 60×3 seamless steel pipe; The end high pile crossbeam adopts H 400×300×10×16, and the middle high pile crossbeam adopts H 300×200×8×12.

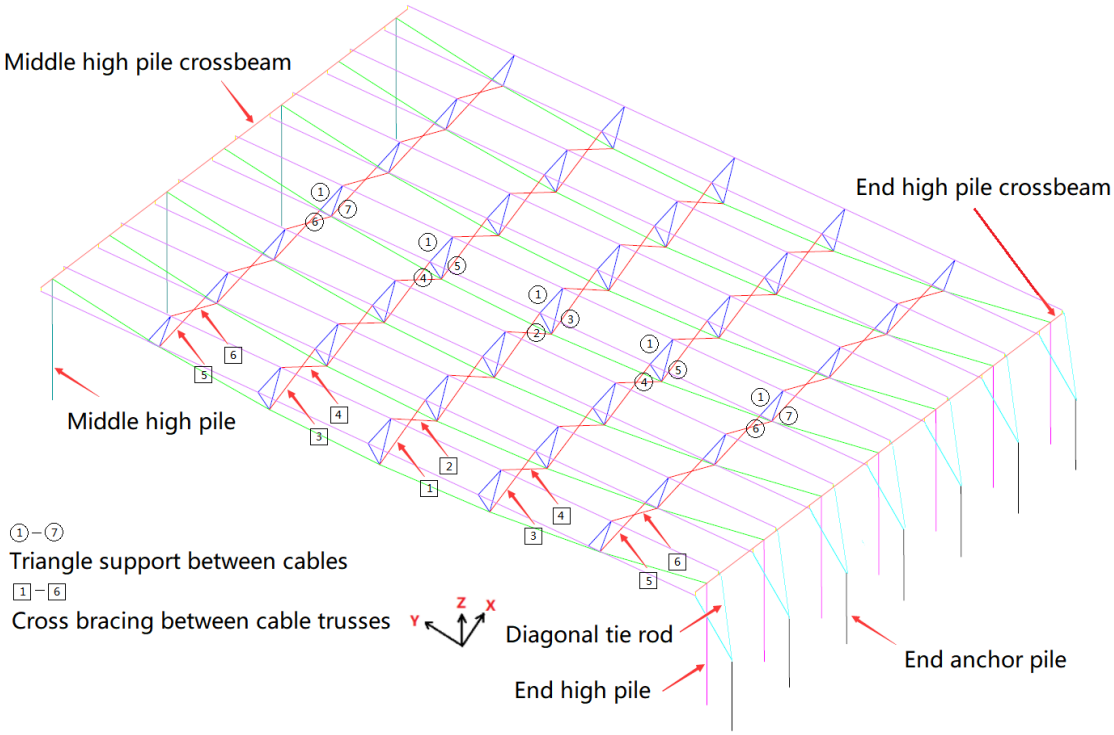

Fig. 8 Layout of photovoltaic power generation bracket components

References

[1] Zhang Zhiping, Guo Liangliang, Wang Qunqing, et al. Key Construction Technology of Cable-stayed Flexible Cable-truss Structure for Cambodia Stadium [J]. Construction Technology. 2020 (22).

[2] Dong Hui, Chen Li, Hong Jian. Dynamic Response Of Protective Door Of New Cable-Membrane Structure [J]. Industrial Construction. 2014 (S1)

[3] Huang Zhenxiong, Wang Haibing, Chen Tao, et al. Research on Construction Technology of Rigid Metal Roof Supported on Flexible Orthogonal Cable Net [J]. Construction Technology. 2018 (02)

[4] Shen Li, Xiong Jiawen, Zhang Guoqiang, et al. Design and application of flexible cableway anchoring system for high-altitude organization based on FAST super large cable Net [J]. Prestress Technology. 2016 (03)

[5] Zhang Cai, Ding Bailong, Zhang Lei, et al. Application of Unit Load Method in Flexible Cable Net [J]. China Construction Metal Structure. 2005 (09).

[6] Zhang Zhiping, Guo Liangliang, Wang Qunqing, et al. Model Test and Engineering Application of Cable-stayed Flexible Cable-truss Structure for Aided Cambodia Stadium [J]. Construction Technology. 2020 (22)